WET OXIDATION OF PHENOL ANALOGUES USING Mn(II)@Silica AS HETEROGENEOUS CATALYST

Vishal J. Mayani[1], Krishna Gopal Bhattacharyy[2] and Suranjana V. Mayani*[3]
[1]*Department of Advanced Materials Chemistry, College of Science and Technology, Dongguk University, Gyeongju, Gyeongbuk 780-714, Republic of Korea*
[2]*Department of Chemistry, Gauhati University, Guwahati 781-014, Assam, India*
[3]*Department of Chemistry, Marwadi University, Rajkot-Morbi Road, P.O. Gauridad, Rajkot 360003, Gujarat, India*
*For correspondence. (suranjana.mayani@marwadieducation.edu.in)

Abstract: Toxic and bio-resistant phenolic compounds are some of the most common hazardous organics in aqueous systems presenting challenging problem in waste water treatment. In the present study, wet oxidation without a chemical oxidant was attempted using Mn(II)@silica as the catalyst. The catalysts were well characterized by physico-chemical characterization methods. The conversion of phenol, 2-chlorophenol and 2-nitrophenol was 89.7, 85.5 and 78.8 % with hydrothermally synthesized Mn(II)@silica, and 94.2, 91.1 and 89.4 % with impregnated Mn(II)@silica, respectively. The reactions followed pseudo first order kinetics. The effects of pH, reaction time, catalyst load, feed concentration, and temperature were investigated. GC-MS analysis showed that the persistent organics were oxidized to simpler end products. Further oxidation is expected lead to complete mineralization of the contaminants. Mn(II) coupled silica was noticed to be a better oxidation catalyst for the organic pollutants than the synthesized Mn(II)@silica.

Keywords: catalysis; wastewater treatment; wet oxidation; Mn(II)@silica; phenols

1. Introduction:

An increasing number of studies have focused on finding efficient, inexpensive and green catalysts for oxidizing persistent organic chemicals to environmentally harmless compounds. Catalytic oxidation has been always preferential [1-3] because the processes can be operated at mild temperatures and pressures with a positive outcome on the economics of treatment. In a homogeneous catalysis process, transition metal complexes are frequently used as homogeneous catalyst. However, its use is still limited because of less stability, difficulties in recovery and reuse. When fine particles of metal oxides are utilized as the catalyst, it accumulated into larger granules as the reaction proceeds, resulting in a rapid decrease in surface area and consequently, catalytic activity. This arisen obstacle can be conquered by allocating the active catalyst on a porous framework, such as charcoal, polymer, clay or zeolite, by impregnation, intercalation, ion exchange, or encapsulation [4]. A mesoporous silica material, MCM-41, is a promising contributor for heterogeneous support for a dispersed active phase because the material possesses a hexagonal array of pores with a large number of surface-SiOH groups and considerably weak acidity. The pores cover a broad spectrum of diameters ranging from 15 to 100 Å, which are controlled by an appropriate choice of template or by the synthesis conditions [5]. The introduction of transition metals, such as Fe, Cr, Cu, Mn or Ti, into porous silica network, has been found to improve the oxidizing ability of the silica material considerably [4-6]. These materials can be obtained by either hydrothermal synthesis or isomorphous substitution, or wet impregnation techniques. The modified preparation method of MCM-41 using effective species associated with the framework strong interactions forms distinct and homogeneous catalytic site in the porous system. The thermal stability of these transition metal-incorporated silica material catalysts have been well established using thermogravimetric-differential thermal analysis (TG-DTA). These catalysts have also been shown to be hydrothermally stable, even though the bimetallic mesoporous materials have greater hydrothermal stability, *i.e*., hydrophobicity, thermal stability and acid strength [7-9]. Srinivas et al. [5] revealed the importance of metal ions associated with the surface of MCM-41 for effective oxidation.

Noxious and bio-resistant phenolic compounds in aqueous system always present a challenging problem in wastewater treatment [3, 10]. These compounds are ubiquitous in waste and natural waters, and may originate from numerous points of supply. The matter of the petroleum processing plants, olive oil production Kraft

pulping, and different chemical industries producing herbicides, phenolic resins, pesticides, paints, solvents, polymers, and other hazardous chemicals are among the prominent water pollutant bodies. Chlorophenols are used widely in numerous applications and the wastewaters generated from such use contaminate the surrounding soil and water courses, affecting public health [11-13]. 2-Chlorophenol is considered as a hazardous compound [14-16]. Electron-withdrawing natures of aromatic nitro compounds prevent chemical or biological oxidation as well as hydrolysis. Dyes, rubber chemicals, paint coloring and mold killing compounds are primarily prepared using nitrophenol analogues. They are also formed in auto exhaust. The fabric industry may also discharge both 2-nitrophenol and 4-nitrophenol into the surface water. In addition, the nitrophenols are found in treated wastewater from the iron and steel manufacturing industries, foundries, pharmaceutical manufacturing and electrical/electronic components production industries. Nitrophenols are also constituents of wastewater from petroleum refineries [17]. Nitrophenols have been identified in the primary and secondary effluent of municipal wastewater treatment plants. Transforming these persistent organics into harmless chemicals cannot be achieved using the conventional biological oxidation process and conventional solvent extraction requires high capital investment and creates the problem of high dissolved solids in the effluent [18, 19].

The present work evaluated the suitability and efficiency of catalysts obtained by incorporating Mn(II) into silica material by direct hydrothermal synthesis (Catalyst C1) and by impregnation (Catalyst C2) with respect to the aqueous oxidation of phenol analogues (phenol, 2-chlorophenol (2-CP) and 2-nitrophenol (2-NP)). The reaction conditions were varied to examine the effects of pH, reaction time, catalyst load, feed concentration, and temperature without the use of a chemical oxidant. The GC-MS analysis of the products and mechanistic pathways were also illustrated.

2. Methods and materials:

2.1. Chemicals:

The chemicals used to prepare the catalysts, $Al_2(SO_4)_3$ $18H_2O$, $MnCl_2$ $4H_2O$, sodium hydroxide, phenol (E. Merck, India), tetraethyl orthosilicate (TEOS, 99 %), ethyl amine (EA, 65%) (Merck-Schuchardt, Germany), tetramethylammonium hydroxide (TMAH), silica gel, (Sigma, U.S.A), cetyltrimethylammonium bromide (CTAB, 99%) (B.D.H. Chemicals, England), hexadecyltrimethylammonium chlorides (HDTMAC), 2-chlorophenol and 2-nitrophenol (Fluka, Switzerland) were used as received. The stock solutions of concentration 10^{-3} M were prepared in double distilled water for each of the reactants.

2.1.1. Hydrothermal synthesis of Mn(II)@silica:

Mn(II)@silica was synthesized hydrothermally followed by Ti(IV)-MCM-41 immobilization method [20]. For this purpose, $MnCl_2$ $4H_2O$ (0.2 g) was used as the metal source and TEOS was used as the organic silicon source. In a Teflon vessel, Mn(II) salt was dissolved in a minimum amount of water (~5 ml) and TEOS (8.96 ml), CTAB (2.9 g), ethylamine (1.33 ml), and tetramethylammonium hydroxide (1.5 g) were added sequentially to this solution with continuous mechanical stirring for 4 h at room temperature. The following composition gel was obtained at pH 11.6: 1.0 TEOS: 0.2 CTAB: 0.02 Mn(II): 0.6 EA: 0.20 TMAH: 150 H_2O. The prepared gel was moved to a Teflon stainless steel autoclave reactor and kept at 373 K for 48 h under autogenous pressure. The resulting product (Catalyst C1) was filtered, washed with distilled water and dried in air for 8 h followed by air calcination at 823 K for 24 h.

2.1.2. Hydrothermal synthesis of MCM-41 and introduction of Mn(II) by impregnation:

The silica material MCM-41 was synthesized [21] by mixing aqueous solutions of aluminium sulphate (0.62 g) and sodium hydroxide (0.3 g) dissolved in a minimal amount of water in a 250 ml Teflon-lined beaker and stirred continuously until a clear solution was obtained. TMAH (9.4 g), silica gel (9.26 g) and HDTMAC (10.55 g) were added slowly with stirring at room temperature. The pH of the resultant solution was kept at 11.0 by NaOH pellets addition. Stirring was continued until a fine gel was obtained. The composition of the gel was: 1.0 SiO_2: 0.27 HDTMAC: 0.06 $Al_2(SO_4)_3$ $18H_20$: 0.03 Na_2O: 0.33 TMAH: 20 H_2O. The formed gel was transferred to a Teflon autoclave reactor and preserved 373 K for 24 h. The porous semi-crystalline silica materials, were recovered by filtration, washed with distilled water, air dried and followed by air calcinations 823 K for 5 h. Mn(II) impregnated silica (Catalyst C2) was prepared by mixing together equal amounts of silica and $MnCl_2$ $4H_2O$, using a minimum volume of water for wetting. The process was followed by solvent evaporation at 393 K for 5 h and air calcination at 773 K for 6 h.

2.2. Catalyst characterization:

The framework of prepared Mn(II)@silica was validated by X-ray diffraction (XRD, Phillips X'pert MPD diffractometer, Almelo, The Netherlands) by comparing with common XRD patterns of MCM-41. The percentage of Mn(II) entering into silica material was determined by atomic absorption spectrophotometry (AAS, Varian SpectrAA220). Associated active groups were classified by KBr self-supported pellet technique of Fourier transform infrared spectroscopy (FTIR, Perkin Elmer Spectrum RXI). The morphology of the catalysts was measured by scanning electron microscopy (SEM, LEO-1430 VP, UK). The thermal stability of the catalysts was determined by thermo- gravimetric analysis (TGA, Mettler Toledo equipment, Model TGA/SDTA 851^e, USA), and measurements of the surface area and pore size by nitrogen adsorption (Micromeritics ASAP-2010, USA) and cation exchange capacities (CECs) using the copper bisethylenediamine complex method [22].

2.3. Oxidation of phenol, 2-CP and 2-NP:

Heterogeneous catalytic oxidation was executed in a high pressure reactor (Toshniwal Instruments, India). The oxidation reaction was carried out using appropriate catalyst load, 50 ml feed volume, 353 K temperature, 0.2 MPa autogenous pressure, 180 rpm stirrer speed and a fixed time interval of 300 min. The phenol, 2-CP and 2-NP concentrations were 10^{-3} M each and the aqueous solution had a pH value of 4.5, 4.3 and 5.2, respectively. The reactant solution pH was differed from 3 to 9 by drop wise addition of 0.1 N HNO_3 (phenol, 2-CP) or HCl (2-NP) or NaOH solutions. Upon completion of reaction, the resultant solution was centrifuged and the remaining unconverted phenol, 2-CP and 2-NP in the supernatant layer were estimated spectrophotometrically (Hitachi UV-visible U3210), at λ_{max} values of 270, 274 and 409 nm, respectively. Calibration curves for the quantification of the results were obtained with a minimum of 5 standards.

Oxidized product identification was accomplished by gas chromatography-mass spectroscopy (GC-MS, Shimadzu GC 2010, USA). The oxidized products were extracted with equal volume chloroform mixing with product solution followed by vigorous shaking and settle down. 0.6 µL extracted product volume was injected in GC-MS analysis each time.

3. Results and discussion:

3.1. Characterization of the catalysts:

The uncalcined silica material showed a prominent peak at 2θ = 2.45° (d = 36.06 Å) succeeded by peaks at 4.15° (d = 21.27 Å) and 4.72° (d = 18.71 Å) (Figure 1). The calcined silica material showed three XRD peaks corresponding to 2θ values of 2.48° (d = 35.57 Å), 4.23° (d = 20.88 Å) and 4.93° (d = 17.91 Å). Liepold et al. [23] reported that silica material MCM-41, has three to five reflections between 2° and 5°. The materials are expected to have long range order due to the hexagonal arrays of parallel silica tubes and are evidenced to the planes (100), (110), (200), (210), and (300) XRD reflections. The comparison of XRD pattern of uncalcined silica material found at 2θ value 2.45, 4.15 and 4.72° corresponding to planes (100), (110), and (200), reflections respectively, it confirmed the our silica material preparation method in the present work. The calcined silica yielded the most prominent diffraction peak at 2θ = 2.48°, which could be evidenced to the plane (100) reflection, the two added peaks at 4.23° and 4.93° were assigned to the planes (110) and (200) reflections. None reflections at higher angles are expected because silica materials are considered as a non-crystalline at atomic level. Supplementary sense for this kind of nature is being structural features having very little influence on the reflections at higher angles and if they present, these reflections are fundamentally very weak to be important. The characteristic planes (100), (110) and (200) reflections for Mn(II) immobilized silica were observed (Figure 1). The 2θ values of hydrothermally synthesized Mn(II)@silica was 2.31° (d = 38.18Å), 3.96° (d = 22.31 Å), and 4.49° (d = 19.67 Å). Furthermore impregnated Mn(II)@silica had 2θ values of 2.39° (d = 36.90 Å), 4.07° (d = 21.70 Å), and 4.68° (d = 18.87 Å). All the reflection bands have shown a minor shift in the case of the catalysts compared to the silica material. Therefore, metal-incorporation has a considerable influence on the structural regularity of the silica materials. The structure and uniformity was noticed intact after immobilization, which was also observed by other workers [5].

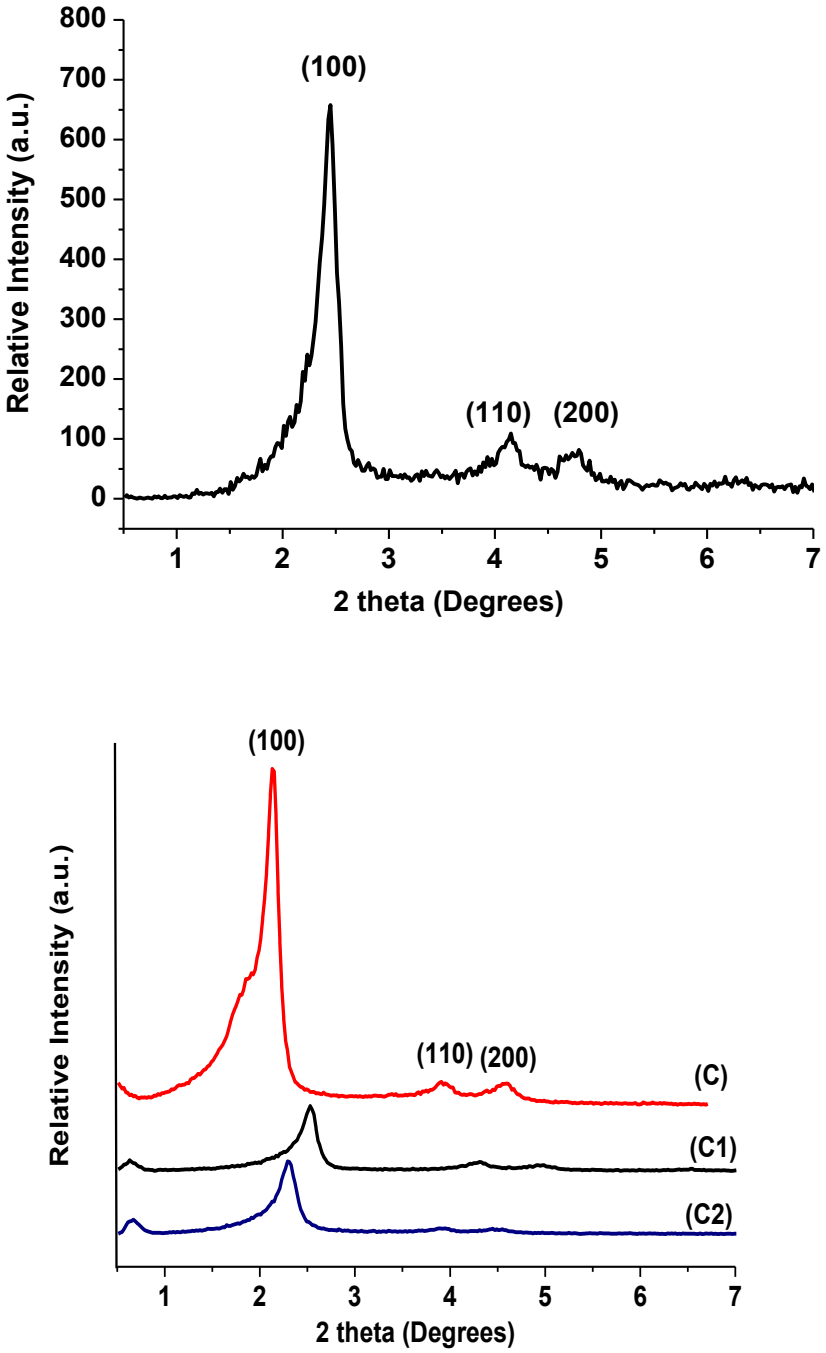

Figure 1: XRD pattern of uncalcined silica (top) and calcined silica, synthesized Mn(II)@silica (C1), and impregnated Mn(II)@silica (C2) (bottom).

SEM (Figure 2) indicated that compared to the parent silica material, the surface topography of Mn(II)@silica showed significant changes regarding whether the sample had been synthesized hydrothermally or obtained by the impregnation technique. In the hydrothermally synthesized Mn(II)@silica, the tendency was to form more small granules on the surface. This tendency increased further in the impregnated Mn(II)@silica and the micrograph indicates that the larger particles of silica material were covered with small granules. In all cases, the surface was not uniform and a large number of faults and crevices could be observed clearly.

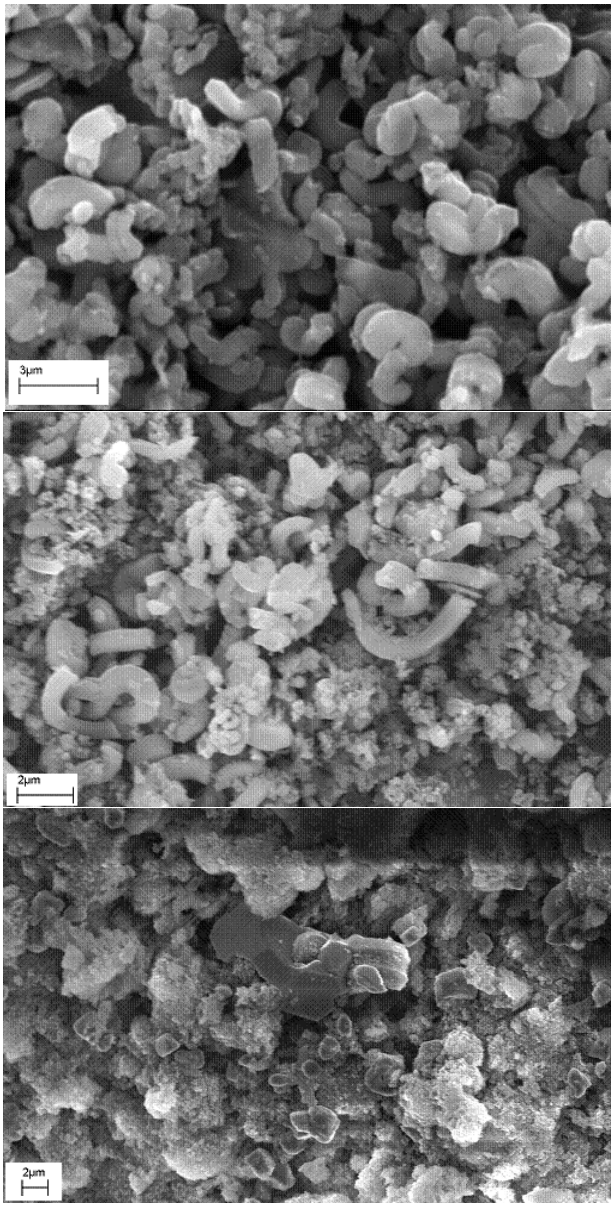

Figure 2: SEM micrographs of silica (top), Mn(II)@silica (synthesized, middle), and Mn(II)@silica (impregnated, bottom).

The uncalcined silica material, calcined silica material and metal incorporated Mn(II)@silica (hydrothermally synthesized) showed a characteristic FTIR band at 960, 965 and 964 cm^{-1}, respectively. Lattice defects and presence of M-O-Si type tetrahedral framework linkages is associated with FTIR band value. A careful examination of this band, revealed a slight red shift in the Mn(II) incorporated samples. Literature report supports the band value assigned to a Si-O vibration in a Si-OH group in siliceous MCM-41 [24]. In this event, it is acceptable to assign the red shift in Mn(II)@silica to the replacement of an OH group by an O-Mn(II) group [5]. The absence of this band value for impregnated Mn(II)@silica is a visible signal of non-penetrate nature of prepared material into framework of silica material by forming O-Mn(II) or identical linkages. The hydrogen-bonded vicinal pairs for silanol groups is the reason for broad absorption value between 3650 and 3400 cm^{-1} in the FTIR spectra (3430 cm^{-1} for the uncalcined silica, 3434 cm^{-1} for calcined silica, 3480 cm^{-1} for hydrothermally synthesized Mn(II)@silica, and 3440 cm^{-1} for impregnated Mn(II)@silica) [23]. The broad band between 1000 and 1250 cm^{-1} for the silica samples (1100 cm^{-1} and 1210 cm^{-1} for uncalcined silica, 1090 cm^{-1} and 1206 cm^{-1} for calcined silica, 1091 cm^{-1} and 1184 cm^{-1} for impregnated Mn(II)@silica, and 1092 and 1213 cm^{-1} for hydrothermally synthesized Mn(II)@silica) are correlated to the asymmetric stretching of Si-O-Si linkage. The FTIR bands at 799 cm^{-1} and 1630 cm^{-1} for uncalcined silica, 794 cm^{-1} and 1637 cm^{-1} for calcined silica, 669 cm^{-1} and 1660 cm^{-1} for hydrothermally synthesized Mn(II)@silica, 669 cm^{-1} and 1626 cm^{-1} for

impregnated Mn(II)@silica are associated to aliphatic C-H bending vibrations as long as the organic template used during the synthesis of silica material. C-H stretching bands were also observed at 2800-3100 cm^{-1} (2923 cm^{-1} for uncalcined silica, 2861 cm^{-1} for impregnated silica and 2930 cm^{-1} for hydrothermally synthesized Mn(II)@silica), which is in agreement with the published results [25]. FTIR spectroscopy revealed an appreciable shift in the characteristic frequencies due to the introduction of Mn(II) into silica. Note that the OH-stretching vibrations corresponding to Bronsted OH groups were absent in silica as well as the two Mn(II)@silica samples in accordance with the very low Bronsted acidity of these materials [7].

The impregnated Mn(II)@silica composite material prepared by adding equal amounts of silica and Mn(II) salt (w/w) and it is found be 1.13 % Mn(II) metal through AAS analysis. The hydrothermally synthesized Mn(II)@silica (0.02 mole) revealed 1.12 % of Mn(II) metal into silica over AAS analysis. Therefore, impregnation can achieve entry of a similar amount of Mn(II) into silica material.

The cation exchange capacities (CECs) of silica material, impregnated and hydrothermally prepared Mn(II)@silica were 0.20, 0.26 and 0.21 meq/g, respectively. Although the differences were small, the incorporation of Mn(II) by impregnation enhanced the CEC considerably. The framework defects and collapsed bonds in the composite surface as well as to structural hydroxyl group transfer activities were generally evaluated by CEC analysis [26]. SEM images exhibited that the surfaces of both impregnated and synthesized Mn(II)@silica had numerous defects and cracks, and that the formation of small granules was higher in case of the impregnated sample. The higher CECs value of impregnated Mn(II)@silica could be one of the reason this characteristics.

The thermo-gravimetric percentage weight loss of calcined silica material, impregnated and hydrothermally developed Mn(II)@silica was 3.12, 2.78 and 6.62 %, respectively, over TGA temperature range between 323 to 1073 K. All the materials have shown greater thermal stability. Indeed, the thermal behavior of the transition metal associated silica composite in air has been built using thermogravimetric-differential thermal analysis (TG-DTA) method [9].

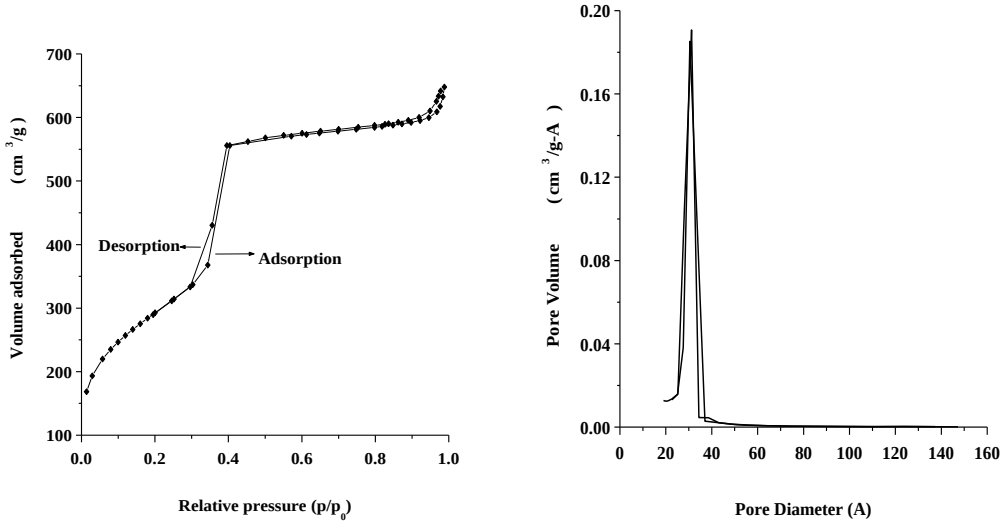

Figure 3: N_2 Adsorption-desorption isotherm and pore diameter and relative pore volume curves of calcined silica.

Table 1 lists the BET surface area, pore volume and pore diameter of the prepared materials. Figures 3 and 4 show the N_2 adsorption-desorption isotherms, pore diameter and relative pore volume. The isotherms belong to type IV according to the IUPAC convention and are typical of mesoporous materials. A linear increase up to a relative pressure of 0.3 indicates nitrogen entering the meso pores to form a monolayer. When p/p_0 is > 0.3, a steep rise occurs due to capillary condensation inside the pores. The subsequent long plateau at higher relative pressures, $0.4 < p/p_0 < 0.8$, indicates N_2 filling up the relatively small pores in a restricted manner. The adsorption again increases at very high relative pressures [27, 28]. The isotherms curves of silica material and transition metal supported silica was similar even though in the latter case, the adsorption rose much more

steeply at a relatively low relative pressure. Notwithstanding, a visible downturn in BET surface area was discovered from 1064 to 720 and 1064 to 771 m^2 g^{-1}, it is result of diverse synthesis methods of the hydrothermally synthesized and impregnated Mn(II)@silica, respectively. A straight decrease in the mesoporous diameter was examined from 35.4 to 32.4 Å and 35.4 to 30.4 for the impregnated and hydrothermally prepared Mn(II)@silica, respectively. A decrease in pore volume from 0.942 to 0.625 and 0.942 to 0.548 cm^3 g^{-1} was also noted for the impregnated and hydrothermally developed Mn(II)@silica, respectively (Table 1).

Table 1: Surface and pore characteristics of calcined silica, hydrothermally synthesized Mn(II)@silica (C1) and impregnated Mn(II)@silica (C2).

Compound	BJH Pore diameter Å	Total Pore volume cm^3 g^{-1}	BET surface area m^2 g^{-1}
Silica	35.4	0.942	1064
Synthesized Mn(II)@silica	30.4	0.548	720
Impregnated Mn(II)@silica	32.4	0.625	771

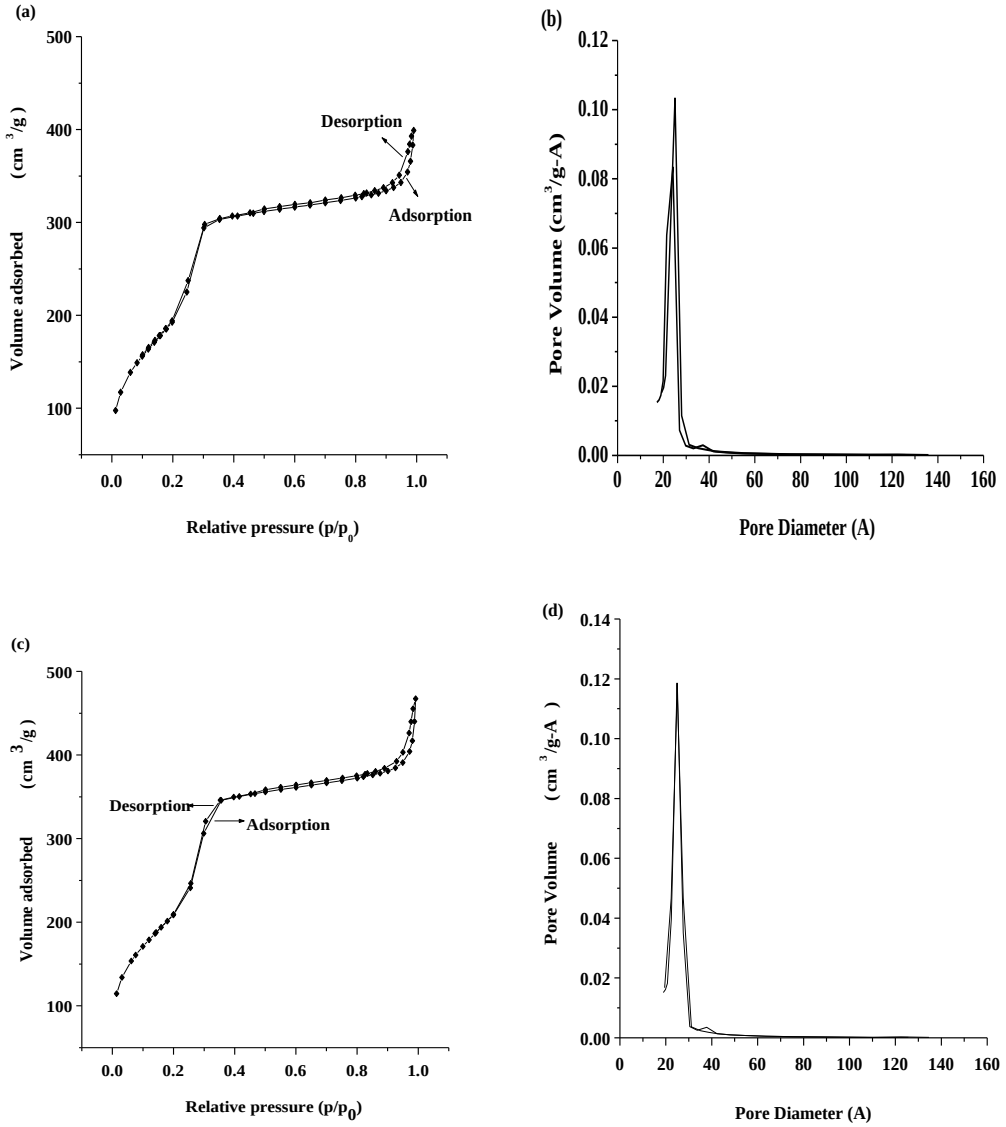

Figure 4: N_2 Adsorption-desorption isotherm and pore diameter and relative pore volume curves of hydrothermally synthesized Mn(II)@silica (C1, (a), (b)) and impregnated Mn(II)@silica (C2, (c), (d)).

3.2. Adsorption experiment:

Phenol, 2-CP and 2-NP were found to adsorb weakly on the Mn(II) incorporated silica material. Separate sets of experiments on the adsorption study of phenol, 2-CP and 2-NP (1 X 10^{-3} M each) on hydrothermally prepared and impregnated Mn(II)@silica using 2.0, 2.5, 3.0, 3.5, 4.0 g L^{-1} catalysts. Adsorption study was conducted by continuously agitating 50 ml of the solution in 100 ml flasks followed by shaking in water bath at 353 K for 300 min under atmospheric pressure. The mixture was centrifuged and the concentration of phenol, 2-CP and 2-NP remaining unadsorbed was estimated in the centrifugate spectrophotometrically. The results were analyzed by a fit to the Langmuir isotherm [$C_e/q_e = 1/(bq_m) + (1/q_m) C_e$], where C_e and q_e are the concentrations of the adsorbate at equilibrium in the liquid phase and the solid phase, respectively. b and q_m are the Langmuir coefficients representing the equilibrium constant for the adsorbate-adsorbent equilibrium and the monolayer capacity. The Langmuir isotherms were linear where regression coefficient R was + 0.91 to + 0.99 and it produced the monolayer capacity q_m in the range of 5.4, 9.4 and 14.1 mg g^{-1} for C1 and 5.5, 17.8 and 13.5 mg g^{-1} for C2 against phenol, 2-CP and 2-NP, respectively. The absorbed amount was discharged by both the catalysts (C1 and C2) when treated with water at the same temperature for 1 h. The value of monolayer capacities proposed that great extent of phenol, 2-CP and 2-NP were held reversibly by adsorption on the prepared catalyst surface. Thus the results are deal for the solids to act as heterogeneous catalysts for the reactions of the compounds and catalyst can be easily separated from liquid phase solution containing reactants and products. This was possible in the present case because Mn(II)@silica does not retain phenol, 2-CP or 2-NP on its surface irreversibly.

3.3. Wet oxidation of phenol, 2-CP and 2-NP:

3.3.1. Blank experiments:

Before examining the effectiveness of the hydrothermally synthesized and impregnated Mn(II)@MCM-41 as solid catalysts for the wet oxidation of phenol, 2-CP and 2-NP in water (1 x 10^{-3} M each), a set of blank experiments were carried out on the following systems:

(i) phenol, 2-CP or 2-NP alone without a catalyst and H_2O_2,
(ii) phenol, 2-CP or 2-NP and H_2O_2 (molar ratio 1:1) without a catalyst ,
(iii) phenol, 2-CP or 2-NP with MCM-41 as the catalyst (2 g/L), and
(iv) phenol, 2-CP or 2-NP and H_2O_2 (molar ratio 1:1) with MCM-41 as catalyst (2 g L^{-1})

under the similar reaction conditions [temperature (353 K), autogenous pressure (0.2 Mpa), stirrer speed (180 rpm), and time interval (5 h)]. No significant conversion was recorded in sets (i) and (iii), nevertheless small conversion was realized in the sets (ii) (phenol 5.0 %, 2-CP 4.8 %, 2-NP 3.0 %) and (iv) (phenol 12.0 %, 2-CP 8.0 %, 2-NP 5.4 %). These blank experiments revealed that phenol, 2-CP and 2-NP were entirely stable when endorsed as set (i), while H_2O_2 delivered only modest decomposition of the reactants in the act of sets (ii) and (iv). The mesoporous material MCM-41 was maintained as a poor catalyst by not carrying any significant catalytic activity of phenol and its two derivatives as shown in set (iii).

3.3.2. Effect of pH:

The analysis results exhibited that the pH of the medium has an influence over the wet oxidative destruction of phenol, 2-CP and 2-NP (Figure 5). The reactions were conducted using specific reaction condition (temperature 353 K, reaction time 300 min, catalyst load 2 g L^{-1}). Most of the phenol (89.7 %) was oxidized at the natural pH (4.5) of the aqueous solution using directly synthesized Mn(II)@silica and 94.2 % was decomposed with impregnated Mn(II)@silica. The conversion increased slowly until neutral conditions (pH = 7.0) were obtained, but the conversion increment were not significant after pH value greater than 7.0.

Both catalysts achieved approximately 85.5 % oxidation of 2-CP by C1 and 91.1% by C2 catalysts at the natural pH (4.3) of the aqueous solution, respectively. The extent of oxidation increased slowly until neutral conditions (pH = 7.0) were obtained, and then, decreased as the solution became alkaline.
Whereas, at 5.2 pH aqueous solution, oxidation conversion of 2-nitrophenol was 78.8 % and 89.4 % over the hydrothermally synthesized and impregnated Mn(II)@silica catalysts, respectively (Figure 5). The oxidation of 2-NP showed a continuous tendency to increase up to pH 9.

Doong et al. [18] explained that the photo-degradation of 2-CP is favored by the higher pH. The effects of pH are determined by several factors, *i.e.*, reactant, catalyst, mechanism of oxidation, and the appropriate reaction

condition. We have studied that heterogeneous catalysts are capable of working over a wide range of pH values. The additional benefit is not need of acid for maintenance of pH to 2.0-3.0 and effective catalytic oxidation can be done over neutral pH 7.0. This reduces the cost and makes handling safe and easy. Egerton et al. [17] reported that if TiO_2 catalyst based photocatalytic oxidation of 2-NP can be accomplished in the pH range 5.2 to 5.8, catalytic degradation rate of 2-NP jumped by ~70 %. But the degradation increased only lightly (~ 10 %) with further increment of pH value from 5.8 to 7.7. These results are consistent with the conclusion reported by Wang et al. [29] that pH 7.0 is the optimum for the oxidation of nitrophenols, but are adverse to the normal decrease in reaction rate alongside pH increment observed by Augugliarno et al. [30]. The contradictory results might be due to the differences in synthesized catalytic material because two different varieties of TiO_2 were used.

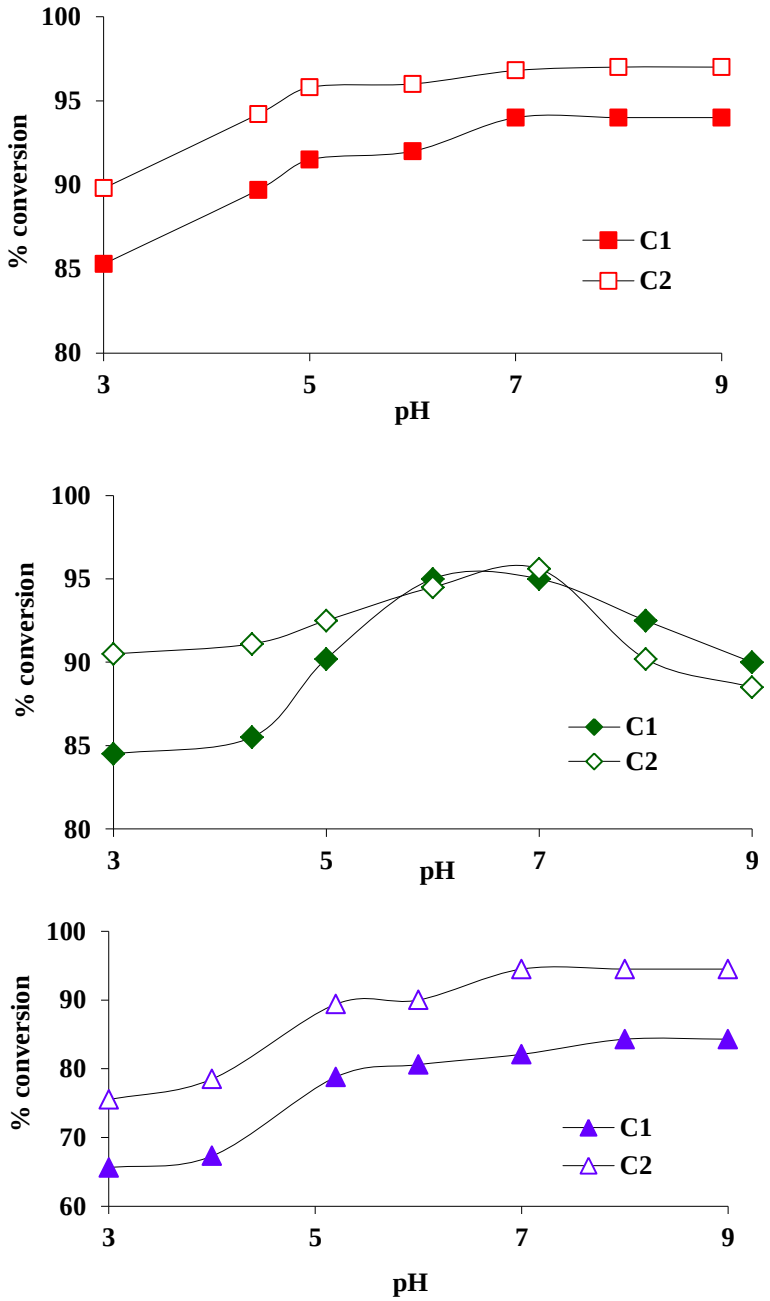

Figure 5: Effects of pH on oxidation of phenol (top), 2-CP (middle) and 2-NP (bottom) with C1 and C2 (synthesized and impregnated Mn(II)@silica) as the catalysts at 353 K (Reaction time 300 min, catalyst load 2 g L^{-1}).

The Mn(II) catalyst leaching possibilities during pH variation was also analyzed by set of experiments, where catalysts were agitated in aqueous medium using specific concentrations (pH 3.0 to 9.0, Temperature 353 K, time 5 h). Leaching was higher at a low pH with the maximum amount of Mn(II) coming out at pH below 3.0. At the natural pH of the aqueous solution of phenol, 2-CP and 2-NP (4.5, 4.3 and 5.2 respectively), It is acceptable leaching results as per World Health Organization (WHO) guideline (Mn(II) in drinking water is 0.4 mg L^{-1}) [31]. Less than 0.3 % Mn(II) had leached into aqueous solution after the completion of reaction using impregnated Mn(II)@silica catalyst, it is giving boost to a Mn(II) concentration of 0.07 mg L^{-1} in the treated aqueous media. Less than 0.5 % Mn(II) leaching occurred for hydrothermally synthesized Mn(II)@silica catalyst and it was identical to a Mn(II) concentration of 0.11 mg L^{-1}. Therefore, leaching does not lead to unacceptable water quality even by the stringent drinking water standards.

3.3.3. Effect of reaction time and kinetics:

The effect of reaction time on total conversion for phenol, 2-CP and 2-NP using both the catalyst C1 and C2 catalysts is given in Figure 6. The catalytic degradation of all three reactants gained with increasing reaction time. Thus, phenol, 2-NP and 2-CP at 353 K shown increased degradation from 35.7-89.7, 38.0-78.8 and 40.3-85.5 % for the catalyst C1 and from 40.5-94.2, 46.0-89.4 and 65.3-91.1 % for the catalyst C2 over the time interval of 15 to 300 min, respectively. The impregnated catalyst C2 is highly active compared to the synthesized catalyst C1. Since, catalyst C2 have generated higher number of active Mn(II) metal on porous framework of silica material compared to counterpart catalyst C1, It makes the impregnated Mn(II)@silica catalyst more productive for the conversion of phenolic compounds.

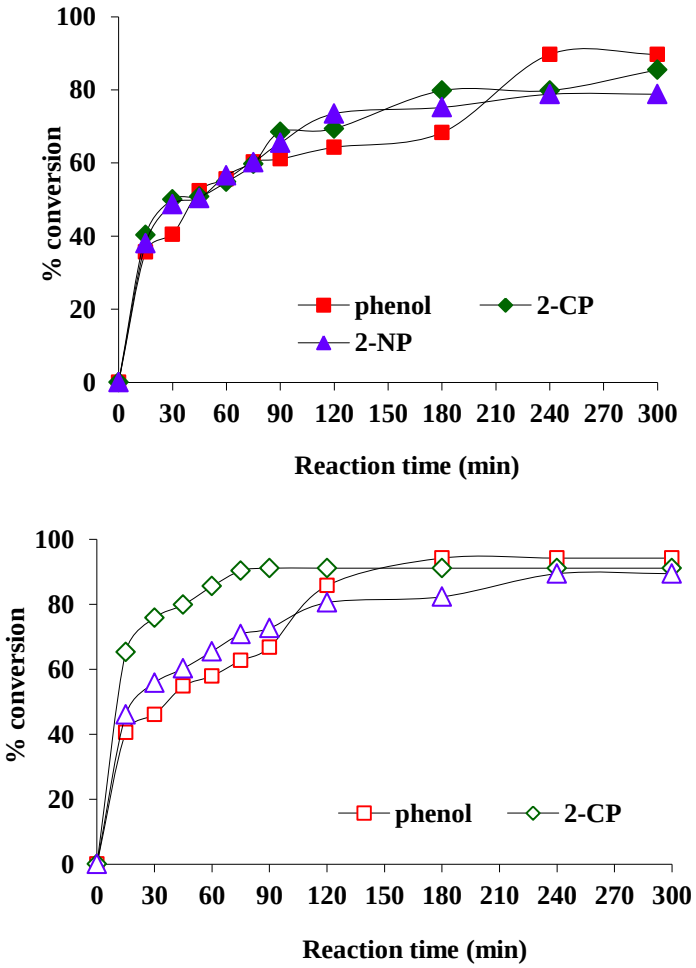

Figure 6: Effects of reaction time on oxidation of phenol, 2-CP and 2-NP with synthesized Mn(II)@silica, C1 (above) and impregnated Mn(II)@silica, C2 (bottom) as the catalysts at 353 K with catalyst load of 2g L^{-1}.

After 300 min reaction time, the overall oxidation followed the order of phenol > 2-CP > 2-NP for both the catalysts although initially (15 min reaction time) the order was 2-CP > 2-NP > phenol for both C1 and C2.

Posada et al. [32] claimed that the complete conversion of 2-chlorophenol was achieved in aqueous medium at 433 K using Cu/CeO_2 catalyst within 130 min. In the present work, the maximum conversion of phenol achieved was 89.7 % with C1 catalyst in 240 min and 94.2 % for C2 catalyst in 180 min at 353 K temperature. Both the catalysts C1 and C2, impregnated and synthesized, were found to be almost comparably active at lower reaction temperature with similar reaction time. And our catalyst, Mn(II)@silica, is economic and eco-friendly compared to commercially available Cu/CeO_2 catalyst.

Using the first order kinetic equation:

$$C_t = C_0 e^{-kt} \quad (1)$$

or,

$$\log C_t = \log C_0 - (k/2.303)t \quad (2)$$

where C_o is the reactant's initial concentration and C_t is the reactant's concentration at time t, the log C_t vs. t plots revealed satisfying linearity (regression coefficient, R = – 0.90 to – 1.00) for our both the catalysts, C1 and C2. Therefore, the catalytic process follows a first order mechanism. The first order kinetic constants have the values for reactants phenol, 2-CP and 2-NP as 6.7 x 10^{-3}, 4.8 x 10^{-3}, and 3.7 x 10^{-3} $Lg^{-1}min^{-1}$ with C1 catalyst and 6.6 x 10^{-3}, 3.9 x 10^{-3}, and 5.8 x 10^{-3} $Lg^{-1}min^{-1}$ with C2 catalyst, respectively. Most of the catalytic reactions are generally best explained by first order kinetics [7] and the wet oxidation of phenol and its two derivatives is no exception. The second order kinetics conformity study was also conducted by plotting the appropriate second order equation, but the plots deviate significantly from linearity and the second order hypothesis was not pursued further.

The kinetic data on the catalytic oxidation of phenol and its derivatives is scarce. Stoyanova et al. [33] reported that Ni-Mn oxide catalyzed (catalyst loading of 2 g L^{-1}) wet air oxidation of phenol has also pursued the first order kinetics along an initial rate coefficient of 22.05 x 10^{-2} min^{-1}. The reaction was very fast with ~ 80 % conversion achieved in 6 min. In the present case, the oxidation of phenol was moderately fast with a rate coefficient almost one order of magnitude lower. It is to be noted that the oxidation rate decreased after 6 min in the case of Stoyanova et al. [33]. First order kinetics was also observed in case of 2,4-dichloro phenol oxidation [34] by Fenton's reagent and 2,4,6 trichloro phenol by ozonation [35].

3.3.4. Effects of reactant concentration:

The conversion of catalytic oxidation was fallen during increase in phenol, 2-CP and 2-NP concentrations at stable catalyst load of 2 g L^{-1} (Figure 7). In the range of five different concentrations, 2 x 10^{-4}, 4 x 10^{-4}, 6 x 10^{-4}, 8 x 10^{-4}, and 10 x 10^{-4} M, the extent of oxidation was 95.0 to 89.7% (for phenol with C1), 98.5 to 94.2 % (for phenol with C2), 94.4 to 85.5 % (for 2-CP with C1), 97.5 to 91.1 % (for 2-CP with C2), 88.8 to 78.8 % (for 2-NP with C1) and 97.1 to 89.4 % (for 2-NP with C2), respectively. The nature of the catalyst and reactants plays significance role in achieving better conversation in reactant concentration study. The negative effect of an increased concentration on the conversion was due likely to the increasing number of reactant molecules flocking together to the catalyst surface competing for the active sites.

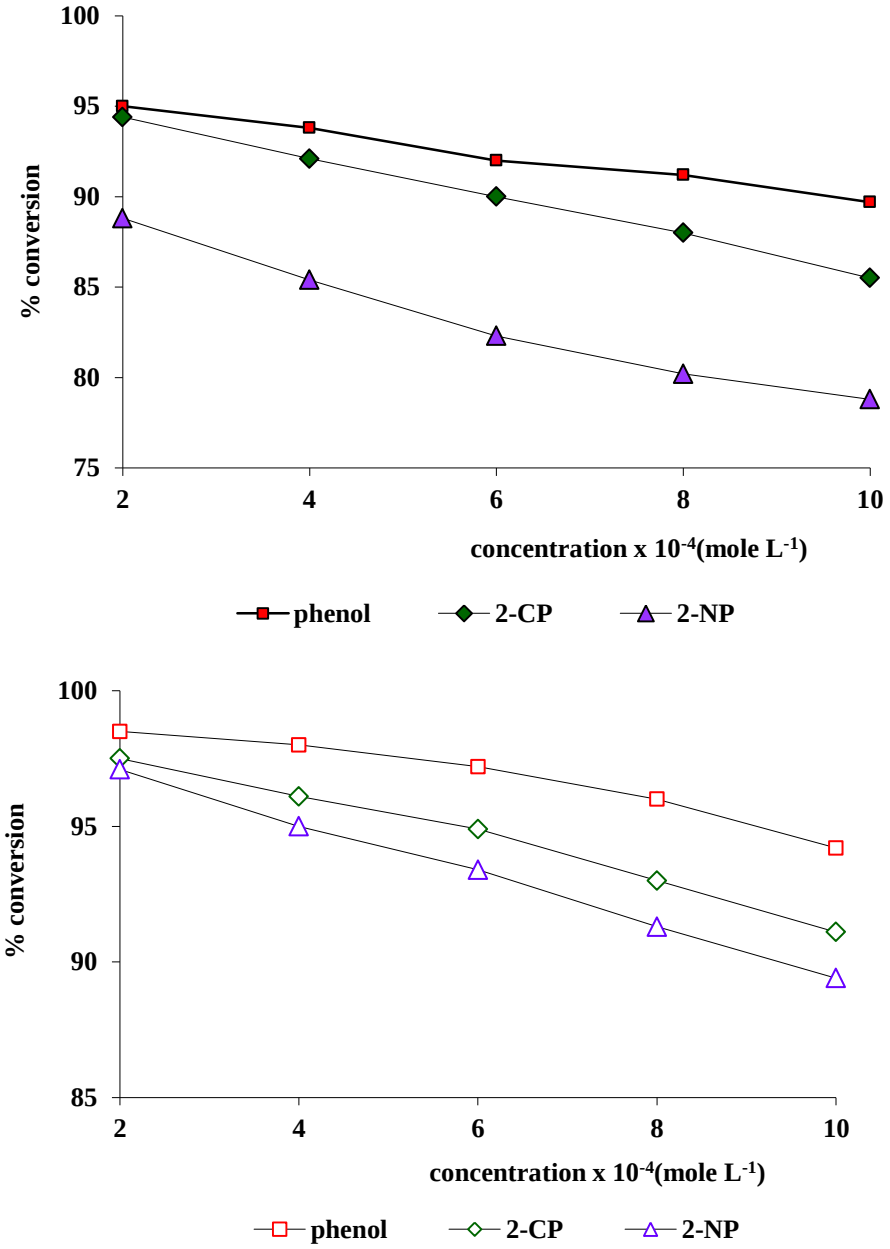

Figure 7: Effects of reactant concentration on oxidation of phenol, 2-CP and 2-NP with hydrothermally synthesized Mn(II)@silica, C1 (above) and impregnated Mn(II)@silica, C2 (bottom) as the catalysts at 353 K (Reaction time 300 min, catalyst load 2 g L^{-1}).

3.3.5. Effects of catalyst load:

Catalyst loading effect was studied by varying five different amount of catalyst 2, 4, 6, 8, and 10 g L^{-1} at a fixed reaction time of 300 min and temperature of 353 K. The results (Table 2) indicated that the catalyst loading had no major influence on the oxidation of phenols.

Table 2: Effects of catalyst load on wet air oxidation of phenol, 2-chlorophenol (2-CP) and 2-nitrophenol (2-NP) at 353 K and reaction time of 300 min.

Catalyst load ($g\ L^{-1}$)	**Total conversion (%)**					
	Synthesized Mn(II)@silica			**Impregnated** Mn(II)@silica		
	Phenol	**2-CP**	**2-NP**	**Phenol**	**2-CP**	**2-NP**
2	89.7	85.5	78.8	94.2	91.1	89.4

4	91.5	85.5	80.2	94.2	95.5	90.0
6	91.5	92.0	80.2	94.2	95.9	90.3
8	91.5	92.0	80.2	94.2	95.9	90.3
10	91.5	92.0	80.2	94.2	95.9	90.3

Using the hydrothermally-synthesized Mn(II)@silica, the oxidation of phenol, 2-CP and 2-NP increased from 89.7 to 91.5 %, 85.5 % to 92.0 % and 78.8 to 80.2 %, respectively, in the range of catalyst loadings of 2 to 10 g L^{-1}. With the impregnated Mn(II)@silica catalyst, the changes in the conversion of phenol, 2-CP and 2-NP in the same range of catalyst loadings were 94.2 % (unchanged), 91.1 % to 95.9 % and 89.4 to 90.3 %, respectively. 2-CP conversion with C1 and phenol conversion with C2 catalysts did not change with increasing in catalyst loadings or with the change in catalyst. Interestingly, well examined tiny amount of catalyst (2 g L^{-1}) could be as precisely active as a large amount in oxidizing the phenols in water almost completely under moderate conditions.

Stoyanova et al. [33] reported that phenol oxidation over a combined Ni-Mn oxide catalyst delivered reaction yield of 28 %, 80 % and 99 % for catalyst loadings of 0.5, 2.0 and 10 g L^{-1} at constant pH 6.0 and a temperature 308 K, respectively, which was attributed to the participation of active oxygen species (O^*) from the catalyst surface in the actual reaction mechanism. The increase in catalyst loading enhances the concentration of active O^* species, consequently, more of the substrate is attacked and converted. In the present study, the catalyst was not a pure oxide, even though some oxide formation is likely during calcination in air. On the other hand, such oxide formation is likely to be limited by the precise locations of Mn(II) ions on MCM-41. Therefore, It can be considered that whatsoever is the catalyst amount (2 g L^{-1} or 10 g L^{-1}), the amount of oxide (and hence the concentration of active O^* species) is similar and hence the conversion did not change much with increasing catalyst loading. The minimum catalyst loading of 2 g L^{-1} has all the active O^* species required for 78-94 % oxidation of the phenols.

3.3.6. Effects of temperature:

The oxidation of phenol and its analogues was carried out at different temperatures (Table 3) from 333 to 413 K in four steps of 20 K increment. The conversion was found to be 85.9-94.0 %, 84.1-86.0 % and 76.8-80.0 % for phenol, 2-CP and 2-NP for the directly synthesized Mn(II)@silica. The corresponding conversions over the impregnated Mn(II)@silica catalyst for phenol, 2-CP and 2-NP were 92.6-95.0 %, 90.0-94.0 %, and 87.9-90.0 %, respectively. This result suggests that the phenol oxidation in aqueous medium water requires inferior energy input and a temperature of 333 K (only 35 degrees above room temperature) was sufficient to induce 76.0 to 92 .0 % oxidation.

Table 3: Effects of temperature on wet air oxidation of phenol, 2-chlorophenol (2-CP) and 2-nitrophenol (2-NP) using catalyst load 2 g L^{-1} in reaction time 300 min.

Temperature (K)	**Total conversion (%)**					
	Synthesized Mn(II)@silica			**Impregnated** Mn(II)@silica		
	Phenol	**2-CP**	**2-NP**	**Phenol**	**2-CP**	**2-NP**
333	85.9	84.1	76.8	92.6	90.0	87.9
353	89.7	85.5	78.8	94.2	91.1	89.4
373	92.3	86.0	80.0	95.0	92.0	90.0
393	94.0	86.0	80.0	95.0	94.0	90.0
413	94.0	86.0	80.0	95.0	94.0	90.0

In the oxidation of styrene by aqueous hydrogen peroxide at 293, 323 and 343 K with MCM41-supported bimetallic catalysts, Parvulescu et al. [8] reported a sudden jump in oxidation conversion was observed using Ru-Cr-MCM-41 catalyst between 293 and 323 K temperature, but Ru-Cu-MCM-41 and Ru-Ni-MCM-41 catalysts did not follow the similar boost. In addition, there was no significant increase in oxidation between 323 and 343 K. In the present work, oxidation was carried out at 333 K and above. Therefore, the results are similar those obtained by Parvulescu et al. [8] even though no hydrogen peroxide was present in the reaction.

3.4. Mechanistic considerations:

The mechanisms for the oxidations of phenol, 2-CP and 2-NP were drawn on the basis of (i) GC-MS analysis of oxidation products after the reaction, (ii) known products of degradation obtained from the literature and (iii) possible products of degradation based on the suggested mechanism.

GC-MS analysis of the product mixtures of phenol in the present study could identify muconic acid, 2,5-dioxo-3-hexenedioic acid and maleic acid. The acrylic acid identified in the products was likely to be one of the end-products of the oxidation of the intermediates. In 2-CP oxidation, two of the critical products identified were pyrocatechol, and 2-chloro-1,4-benzoquinone. Similarly, the products, 2-nitrohydroquinone and 2-nitro-1,4-benzoquinone were found in the product mixture of 2-NP oxidation.

Most established reaction mechanism is predicted on the basis of •OH radicals function as the true oxidizing agent, as in the case of general oxidation reactions, where hydrogen peroxide is the oxidizing agent. The •OH radicals in the present study are likely to have their sources in the metal oxides formation process *i.e.* calcination of the catalysts. The production of •OH radicals on the catalyst will pursue from the interactions between excited the O-atoms of the catalyst and the H-atoms cleaved from the substrate (from phenol, chlorophenol, nitrophenol or water molecule because the oxidation reactions were carried out in aqueous solutions) [33]. The involvement of dissolved oxygen in •OH radical formation is not common because this will result in a drastic decrease in oxidation with increasing reaction temperature (consequent decrease in dissolved oxygen level). Based on the end products and the various intermediates reported by various workers [36], a probable reaction mechanism for phenol degradation could be suggested as in scheme 1. An electrophilic •OH group was added to the aromatic ring of the phenol (I) at *o*- or *p*-position, forwarding to the formation of catechol (II) and hydroquinone (III). Upon further oxidation, catechol is converted to *o*-benzoquinone (IV) and hydroquinone to *p*-benzoquinone (V). The quinones are oxidized easily to the corresponding dicarboxylic acids, *o*-benzoquinone to muconic acid (VI) and *p*-benzo-quinone to 2,5-dioxo-3-hexenedioic acid (VII). Both VI and VII produce maleic acid (VIII), which then decompose to oxalic acid (IX), formic acid (X), acrylic acid (XI), malonic acid (XII), and acetic acid (XIII). In absence of additional radical challengers in the aqueous medium, these lower molecular organic acids can be mineralized gradually to carbon dioxide, the ultimate oxidation product.

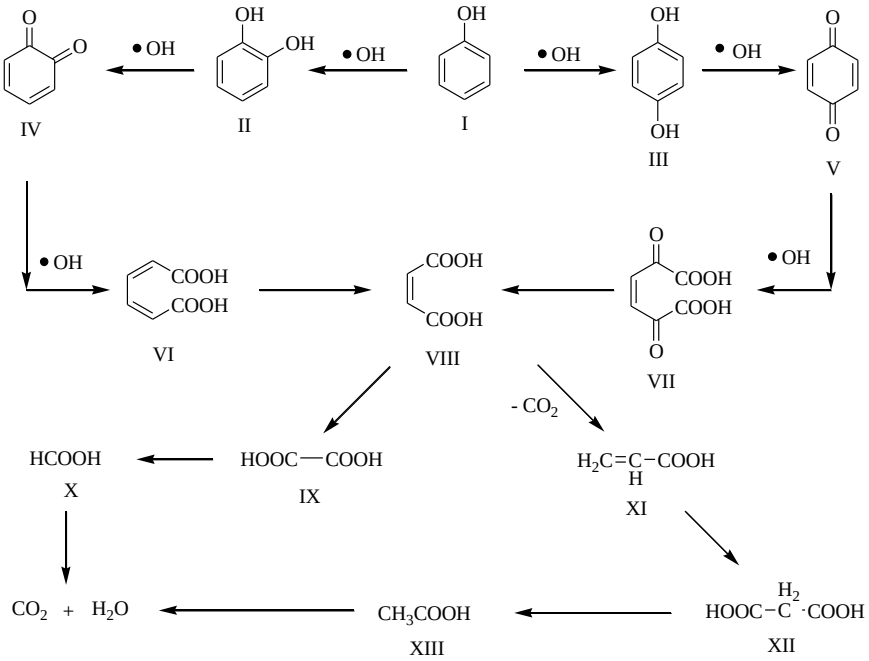

Scheme 1: Degradation pathway of phenol.

The oxidative decomposition of 2-CP [37] is also likely to proceed via hydroxyl radicals produced under the influence of the catalysts. The probable mechanism is based on •OH radicals attacking and substituting the Cl-atoms (scheme 2). The attack by the •OH radical converts 2-CP to a substituted hydroxycyclohexadienyl (HCHD) radical. In the simplified mechanism for the catalytic degradation of 2-CP (I), the addition of •OH to

the aromatic ring leads to the formation of a chlorodihydroxycyclo-hexadienyl radical (ClDHCHD, II), which may disproportionate into 2-CP and chlorohydro-quinone (III), or to simply chlorohydroquinone if the addition is at the *p*-position, or to pyrocatechol (IV) if the addition is at the *o*-position (scheme 2). In the alternative route, ClDHCHD (II) can be converted to 2-chloro-1,4-benzoquinone (V) through water elimination/H^+ abstraction. The aromatic intermediates may be oxidized further, culminating in ring opening and the formation of carboxylic acids and hydroxylated carboxylic acids.

A probable pathway for the oxidation of 2-NP (+I) initiated by Mn(II)@silica catalysts could have proceeded via hydroxyl radicals (scheme 3). The radicals will add to 2-NP (I) at the *p*-position of the cyclic ring to give 2-nitrohydroquinone (II). The product (II) is converted by more hydroxyl radicals to 2-nitro-1,4-benzoquinone (III). This undergoes further transformation through ring cleavage and subsequent degradation to simple aliphatic compounds, which will eventually decompose to CO_2, H_2O, HNO_2, and HNO_3. Najjar et al. [38] suggested an identical scheme for photocatalytic degradation of 2-NP using copper doped Al-pillared montmorillonite.

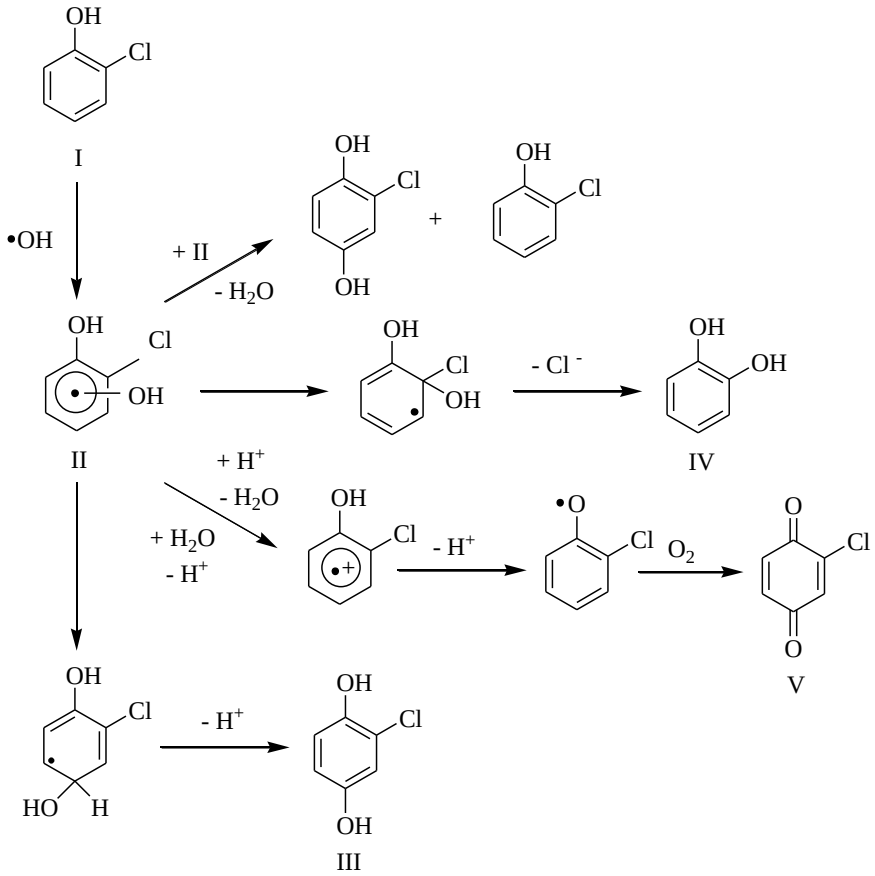

Scheme 2: Degradation pathway of 2-CP.

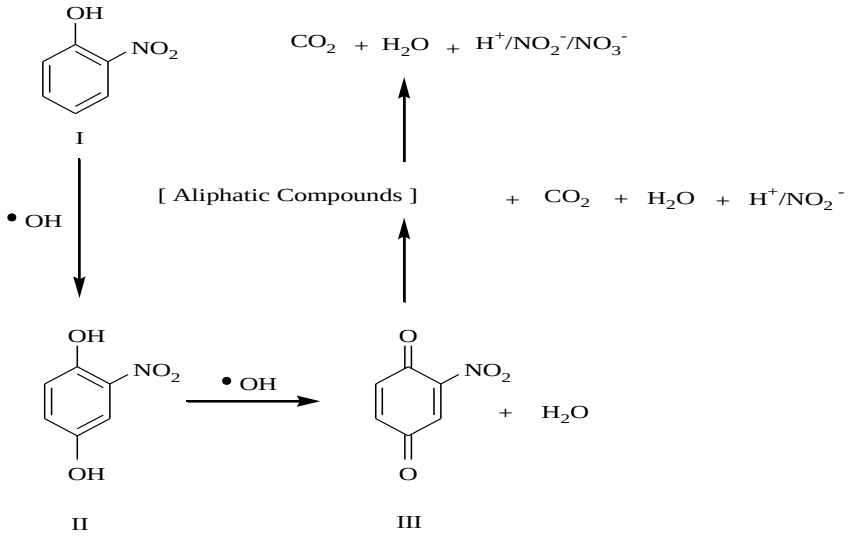

Scheme 3: Degradation pathway of 2-NP.

The stoichiometric equations for the complete mineralization of the phenols can be written as

$$\text{Phenol: } C_6H_5(OH) + 28\ OH \rightarrow 6\ CO_2 + 17\ H_2O \quad (3)$$

$$\text{2-CP: } C_6H_4Cl(OH) + 26\ OH \rightarrow 6\ CO_2 + 15\ H_2O + HCl \quad (4)$$

$$\text{2-NP: } 2\ C_6H_4(NO_2)(OH) + 54\ OH \rightarrow 12\ CO_2 + 31\ H_2O + HNO_3 + HNO_2 \quad (5)$$

requiring 28, 26 and 27 equivalents of •OH for the complete oxidation of one equivalent of phenol, 2-chlorophenol and 2-nitrophenol, respectively. This shows that complete oxidation will require the participation of a large number of active oxygen species (and •OH radicals) on the catalyst surface, which will act as a limiting factor in the reactions.

4. Conclusions:

The introduction of the transition metal Mn(II) into silica material through both hydrothermal and impregnation methods produced very active and effective catalysts for the oxidation of phenol, 2-chlorophenol and 2-nitrophenol. The catalysts could achieve maximum conversion within a short span of 180 to 240 min. The catalytic reactions followed pseudo first order reaction kinetics. The impact of pH and temperature was not uniform in all the catalytic reactions. The pH of the medium influences the oxidation process and the oxidation of 2-CP was not favored at an alkaline pH, whereas phenol and 2-NP oxidation showed an increasing trend at pH > 7.0. GC-MS findings suggested that the steady pollutants were catalyzed to simpler final products such as muconic acid, 2,5-dioxo-3-hexenedioic acid, maleic acid, acrylic acid, pyrocatechol, 2-chloro-1,4-benzoquinone, 2-nitrohydroquinone and 2-nitro-1,4-benzoquinone, considering all three reactants. Further oxidation would lead to complete mineralization of contaminants. The prepared impregnated catalyst (Mn(II)@silica) was act to be a improved oxidation catalyst for the organic pollutants compared to the synthesized Mn(II)@silica catalyst.

Acknowledgments:

This work was supported by Gauhati University (India) research fund, Dongguk University (Gyeongju, South Korea) research fund and Marwadi University, Rajkot, India.

References:

[1] Melero, J.A. et al. “Nanocomposite Fe_2O_3/SBA-15: An efficient and stable catalyst for the catalytic wet peroxidation of phenolic aqueous solutions”. *Chem. Eng. J.* 131 (2007): 245-256.
[2] Xia M. et al. “A highly active bimetallic oxides catalyst supported on Al-containing MCM-41 for Fenton oxidation of phenol solution.” *App. Catal. B: Environ.* 110 (2011):118-125.

[3] Hosseini, S.A.; Davodian, M.; and Abbasian, A.R. "Remediation of phenol and phenolic derivatives by catalytic wet peroxide oxidation over Co-Ni layered double nano hydroxides", *J. Taiwan Inst. Chem. Eng.* 75 ((2017): 97-104.
[4] Norena-Franco L. et al. "Selective hydroxylation of phenol employing Cu–MCM-41 catalysts". *Catal. Today*, 75 (2002): 189-195.
[5] Srinivas, N. et al. "Liquid phase oxidation of anthracene and trans-stilbene over modified mesoporous (MCM-41) molecular sieves", *J. Mol.Catal. A: Chem.* 179 (2002): 221-231.
[6] Jiang, Y. et al. "Fe-MCM-41 nanoparticles as versatile catalysts for phenol hydroxylation and for Friedel–Crafts alkylation". *App. Cata. A: General.* 445-446 (2012): 172 -179.
[7] Szegedi, A. et al. "Spherical mesoporous MCM-41 materials containing transition metals: synthesis and characterization". *App.Catal. A: General.* 272 (2004): 257-266.
[8] Parvulescu, V.; Anastasescu, C.; and Su, B.L. "Bimetallic Ru-(Cr, Ni, or Cu) and La-(Co or Mn) Incorporated MCM-41 Molecular Sieves as Catalysts for Oxidation of Aromatic Hydrocarbons". *J. Mol. Catal. A: Chem.* 211 (2004): 143-148.
[9] Selvaraj, M. et al. "Synthesis and characterization of Mn–MCM-41and Zr–Mn-MCM-41". *Microporous Mesoporous Mater.* 78 (2005): 139-149.
[10] Santos, I. D. dos; Afonso, J.C.; and Dutra, A. J. B. "Electrooxidation of Phenol on a Ti/RuO2 Anode: Effect of Some Electrolysis Parameters". *J. Brazilian Chem. Society*. 22, (2011): 875-883.
[11] Aksu, Z.; and Yener, J.A. "A comparative adsorption/biosorption study of mono-chlorinated phenols onto various sorbents". *Waste Manag.* 21 (2001): 695-702.
[12] Gupta, S.S. et al. "Rapid total destruction of chlorophenols by activated hydrogen peroxide". *Science.* 296 (2002): 326-328.
[13] Pera-Titus, M. et al. "Degradation of chlorophenols by means of advanced oxidation processes: a general review" *App. Catal. B: Environ.* 47 (2004): 219-256.
[14] Jusoh, R. et al. Erratum to "Photodegradation of 2–chlorophenol over colloidal α–FeOOH supported mesostructured silica nanoparticles: Influence of a pore expander and reaction optimization". *Separation Purification Technol.* 149 (2015): 55-64.
[15] Duan, X. et al. "Fabrication of a novel PbO_2 electrode with a graphene nanosheet interlayer for electrochemical oxidation of 2-chlorophenol". *Electrochimica Acta.* 240, (2017): 424-436.
[16] Mangrulkara, P. A.; Kamblea, S. P.; Meshramb, J.; and Rayalua, S. S. "Adsorption of phenol and o-chlorophenol by mesoporous MCM-41", *J. Hazard. Mater.* 160 (2008): 414 -421.
[17] Egerton, T.A. et al. "The effect of UV absorption on the photocatalytic oxidation of 2-nitrophenol and 4-nitrophenol" *J. App. Electrochem.* 35 (2005): 799-813.
[18] Doong, R.A.; Maithreepala, R.A.; and Chang, S.M. "Heterogeneous and homogeneous photocatalytic degradation of chlorophenols in aqueous titanium dioxide and ferrous ion", *Water Sc. Technol.* 42 (2000): 253-260.
[19] Le, X. et al. "Fibrous nano-silica containing immobilized Ni@Au core–shell nanoparticles: A highly active and reusable catalyst for the reduction of 4-nitrophenol and 2-nitroaniline." *J. Mol.Catal. A: Chem.* 395 (2014): 58-65.
[20] Luo, Y. et al. "Study on Ti-MCM-41 Zeolites Prepared with Inorganic Ti Sources: Synthesis, Characterization and Catalysis", *Catal. Comm.* 3 (2002): 129-134.
[21] Beck, J.S. et al. "A new family of mesoporous molecular sieves prepared with liquid crystal templates", *J. Am. Chem. Soc.* 114 (1992): 10834-10843.
[22] Bergaya, F.; and Vayer, M. "CEC of clays: Measurement by adsorption of a copper ethylenediamine complex", *App. Clay Sc.* 12 (1997): 275-280.
[23] Liepold, A. et al. "Textural, structural and acid properties of a catalytically active mesoporous aluminosilicate MCM-41" *J. Chem. Soc. Faraday Trans.* 92 (1996): 4623-4629.
[24] S. Schwarz, D.R. Corbin, and A.J. Vega, In R.F. Lobo, J.S. Beck, S.L. Suib, D.R. Corbin, M.E. Davis, L.E. Iton, and S.I. Zones, (Eds.), Materials Research Society symposium proceedings. Materials Research Society, Pittsburg, PA, 431, p. 137 (1996).
[25] Koh, C.A.; Nooney, R.; and Tahir, S. "Characterisation and catalytic properties of MCM-41 and Pd/MCM-41 materials". *Catal. Letter*, 47 (1997): 199-203.
[26] Rodrigues, M.G.F. "Physical and catalytic characterization of smectites from Boa-Vista, Paraiba, Brazil. Ceramica". 49 (2003): 146-150.
[27] Zheng, S. et al. "Synthesis, characterization and photocatalytic properties of titania-modified mesoporous silicate MCM-41". *J. Mater. Chem.* 10 (2000): 723-727.

[28] Shylesh, S.; and Singh, A.P. "Vanadium containing ordered mesoporous silicates: Does the silica source really affect the catalytic activity, structural stability, and nature of vanadium sites in V-MCM-41". *J. Catal.* 233 (2005): 359-371.
[29] Wang, K.H.; Hsieh, Y.H.; and Chen, L.J. "The heterogeneous photocatalytic degradation, intermediates and mineralization for the aqueous solution of cresols and nitrophenols", *J. Hazard. Mater.* 59 (1998): 251-260.
[30] Augugliaro, V. et al. "Photocatalytic degradation of nitrophenols in aqueous titanium dioxide dispersion". *App. Catal.* 69 (1991): 323-340.
[31] Guidelines for Drinking-water Quality (First Addendum to Third Edition) Volume 1: Recommendations. Geneva: World Health Organization, pp. 595 (2006).
[32] Posada, D. et al. "Catalytic wet air oxidation of Aqueous solutions of substituted phenols". *Catal. Letters.* 106 (2005): 81-88.
[33] Stoyanova, M.; Christoskova, St.; and Georgieva, M. "Mixed Ni-Mn-oxide systems as catalysts for complete oxidation: Part II. Kinetic study of liquid-phase oxidation of phenol", *App. Catal. A: General*, 249 (2003): 295-302.
[34] Oliveira, R. et al. "Experimental Design of 2,4-Dichlorophenol Oxidation by Fenton's Reaction", *Ind. Eng. Chemistry Res.* 45 (2006): 1266-1267.
[35] Benitez, F.J. et al. "Chemical Decomposition of 2,4,6-Trichlorophenol by Ozone, Fenton's Reagent, and UV Radiation" *Ind. Eng. Chem. Res.* 38 (1999): 1341-1349.
[36] Santos, A. et al. "Route of the catalytic oxidation of phenol in aqueous phase", *App. Catal. B: Environ.* 39 (2002): 97-113.
[37] Ilisz, I. et al. "Removal of 2-chlorophenol from water by adsorption combined with TiO_2 photocatalysis". *App. Catal. B: Environ.* 39 (2002): 247-256.
[38] Najjar, W. et al. "Kinetic study of 2-nitrophenol photodegradation on Al-pillared montmorillonite doped with copper". *J. Environ. Monitoring*, 3(6) (2001): 697-701.